MINERALOGIA POLONICA
Vol. 13, No. 1 — 1982

Włodzimierz KOWALSKI, Ilona ŚMIETAŃSKA**

GORCEIXITE FROM A BARITE-FLUORITE DEPOSIT AT STANISŁAWÓW (KACZAWSKIE MTS.)

UKD 549.755.34.08 gorceizyt: 549.905.3:553.689.2'634.1.068.4(438-14 Góry Kaczawskie, Stanisławów)

Abstract. Chemical and mineralogical studies have revealed the presence of gorceixite in the weathering zone of a barite-fluorite deposit at Stanisławów. It has been identified as barium-aluminium gorceixite containing only slight admixtures of Ca and Sr. Gorceixite forms aggregates of fine-crystalline grains intergrowing with quartz. The aggregates have an increased Ti content. Gorceixite from Stanisławów occurs in paragenesis with iron oxides and hydroxides, automorphic barite, manganese minerals of the hollandite-coronadite type, and lithiophorite. It has been found that gorceixite formed in an oxidizing environment at pH 6—8 and at a temperature of 30—50°C.

INTRODUCTION

The hydrothermal barite-fluorite deposit at Stanisławów, regarded to be of the post-Variscan age (Kowalski 1977), lies in a tectonic zone (general strike NW-SE) with older foundations, rejuvenated several times. The zone in question occurs within the Lower Palaeozoic formations of the NE part of the Kaczawskie Mountains (Jerzmański 1965, Paulo 1972, 1973). The rocks of the tectonic zone are intensely brecciated and richly mineralized compared with the rocks outside the zone. They are chlorite-sericite-epidote-quartz metamorphic schists, as well as diabases and metadiabases. The hydrothermal mineralization processes that operated on a large scale in the zone involved carbonatization, silicification, haematitization and pyritization. The vein barite-fluorite mineralization was the final stage of hydrothermal processes in the zone in question (Paulo 1972).

The barite-fluorite vein has a high dip of 70—80° to SW. It is made up of barite, fluorite and quartz, the content of fluorite increasing with depth at the expense of barite (Paulo 1972). These principal components are accompanied by siderite, sometimes appearing in substantial amounts, and subordinate sulphides, mainly pyrite and galena (Jerzmański, Kornaś 1970; Karwowski, Kowalski 1981).

From the viewpoint of mineralogy and secondary processes occurring in the deposit, worth studying is its upper part, which was subject to intense weathering due

* Institute of Geochemistry, Mineralogy and Petrography, Warsaw University, Warszawa, Al. Żwirki i Wigury 93.

to its tectonic structure. The weathering processes gave rise to mineral parageneses of iron oxides and hydroxides and manganese oxides and oxyhydroxides. The manganese parageneses were studied by Kowalski (1967), Bolewski, Fijał et al. (1969), Chrostowska (1970), Paulo (1972), Kowalski and Chrostowska (1982).

MINERAL PARAGENESES OF THE WEATHERING ZONE

Weathering processes were particularly intense in the NW part of the deposit. Barren rocks in the altered tones are generally red, illitized and partly kaolinitized, showing a decreased content of carbonates and sulphides. The secondary processes in the barite vein itself are pronounced down to a depth of 150 m, but in some parts of the deposit they toom place at a depth of about 400 m (Kowalski 1980). The barites of the weathering zones differ from primary barites. They are generally red or rust-coloured, less compact, porous, with typical cavities after leached fluorite. The ores contain neither siderite nor sulphides, as these have been decomposed.

The cavities formed within the deposit have been filled up with secondary minerals. The largest concentrations of these minerals have been found in the NW part of the deposit, at a depth of 100—120 m. The concentrations of manganese minerals reported from mine workings form large nests up to 10—15 m in length, 2 m in thickness, and considerable extension along the dip of the deposit. In all these concentrations manganese minerals are generally separated from iron minerals, their concentration having proceeded either in different places or in succession. In the latter case, manganese minerals are posterior.

Iron minerals form a variety of incrustations, mainly on barites, or irregular concentrations resembling slags or sinters. They are dark, nearly black in colour, hard and porous. Manganese minerals appear in the form of loose, dark, nearly black substance dispersed through weathered barite, or, most commonly, form reniform, nodular concentrations sometimes up to 20 cm in diameter. According to Bolewski et al. (1969), hollandite-psilomelane and lithiophorite-elizawetinskite, accompanied by goethite, barite and metahalloysite-kaolinite occur in the manganese concentrations. The cited authors are of the opinion that the succession of these minerals is difficult to establish and requires more detailed studies. Paulo (1972) also described coronadite-hollandite from the concentrations in question.

The studies carried out in the Institute of Geochemistry, Mineralogy and Petrography of the Warsaw University (Kowalski 1967, 1977, 1980; Chrostowska 1970; Kowalski, Chrostowska 1982) have revealed the presence of hollandite-coronadite, lithiophorite, barite, quartz and goethite in the weathering zone of the Stanisławów deposit. It is also conceivable that braunite, polianite and hausmannite are present. Kaolinite, on the other hand, has not been detected. Worth noting is the increased content of P_2O_5 in the manganese and iron parageneses, varying as a rule from 0.45 to 1.15%. In the brecciated parts of manganese ores co-occurring with a beige-brown-yellowish substance, the P_2O_5 content has been found to increase markedly, running up to 25% in the isolated yellowish concentrations. An increased phosphorous content has also been noted in iron concentrations and in the loose black-greenish substance. Tentative X-ray investigations have shown the presence of svanbergite or phosphates of the gorceixite-crandallite group.

Phosphate minerals occur primarily at the base of manganese reniform concentrations (Phots. 1, 2, 3) which are generally brecciated. The nests of beige-brown-yellowish phosphate substance up to 3—5 cm in diameter are irregularly distributed. Their colour depends largely on the coexisting iron oxide minerals.

EXPERIMENTAL AND RESULTS

Mineralogical and geochemical investigations were carried out on 25 samples representing different forms of concentration of phosphate minerals, particularly their largest aggregates at the base of brecciated reniform manganese concentrations. Macroscopic examination has hown that phosphates coexist with manganese minerals and less commonly, with barite of younger generation. The phosphate substance is friable, of medium hardness, rough to the touch, amorphous, showing similarity to weathering waste resembling clay.

It was impossible to obtain pure, homogeneous phosphate substance for mineralogical and geochemical studies. Therefore, the investigations were performed on phosphate concentrates after larger grains of manganese minerals, quartz, and in some samples also barite had been removed mechanically. The purification of concentrates in bromoform failed to produce the desired effect.

Various methods were used for the identification of phosphates.

Optical examination of this sections has shown that the phosphate in question occurs in association with quartz, manganese and iron oxides, and sometimes with barite. Clay minerals have not been detected. The phosphate usually forms the cement of corroded, hypautomorphic quartz grains (Phots. 4,5). Phosphate grains coat quartz as if corroding it in places, or form random aggregates. They are very fine-crystalline, of the order of thousandth and hundredth parts of a mm. Phosphate crystals show a prismatic or tabular habit, generally being hexagonal or rhombohedral in cross-section. Larger crystals exhibit a zonal structure. In this section the phosphate is colourless, transparent, non-pleochroic, showing a relatively low birefringence of 0.01 and mean refractive index of 1.62. It is characterized by straight extinction with respect to prismatic elongation and does not show any evidence of cleavage. Its optical sign is positive, and it may be uniaxial or biaxial with a very low value of 2V angle.

The habit of phosphate grains and the nature of its aggregates are well illustrated by photomicrographs taken with a Tesla BS-300 scanning microscope (Phots. 6, 7, 8). Crystals with a tabular habit visible on the micrographs (Phot. 6) seem to be indicative of trigonal symmetry (Phots. 7, 8).

Chemical investigation. The chemical composition of phosphate was determined using the methods of classical chemical analysis, electron microprobe analysis and spectroscopic analysis.

Chemical methods revealed that phosphate concentrates contained on the average 10% of insoluble parts (in a mixture of concentrated HCl and HNO_3 acids), P_2O_5 up to 28.0%, and substantial amounts of Al_2O_3 and BaO. Besides these principal components, CaO, MgO, varying contents of iron, a small amount of fluorine and trace amounts of chlorine were detected. Quartz was the dominant component of insoluble parts. In barite-free samples no SO_4^{2-} ions were detected, in spite of the fact that BaO content in the concentrates was high.

Microprobe analysis was carried out on a Link X-ray microanalyser operating in conjunction with a JEM-100C electron microscope and a scanning attachment. The spectrum was recorded at X-ray emission between O and 20 keV and at an electron beam energy of 40 keV. Elements with atomic numbers higher than 11 were determined.

Analysis was made on mineral fragments separated from the thin sections prepared for microscopic examination in transmitted light. The fragments were taken from those places in which the phosphate studied was the principal component. It is conceivable, however, that in some fragments phosphate coexisted with quartz

and iron and manganese oxides. Barite was not detected by microscopic method. Samples to be analysed were fixed to the probe holder with silver paste and coated with a layer of carbon about 100 Å thick. Analysis was carried out in a microarea of about 150 μm^2.

A few X-ray spectra are shown in Fig. 1. As is evident from the figure, Ag and Cu peaks are pronounced in all the spectra. Though these elements may have been present in the samples, which fact was actually confirmed by X-ray spectrophotometry,

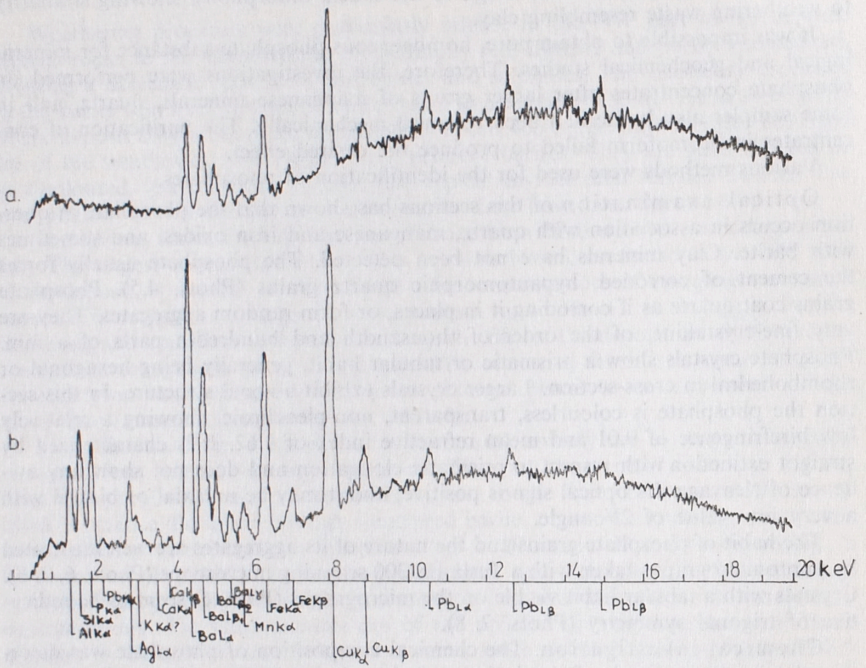

Fig. 1. X-ray spectra of minerals of the gorceixite paragenesis

the Ag peak is to be attributed primarily to silver paste, and the Cu peak to the sample holder.

Since it was presumed that svanbergite, $SrAl_3(PO_4)(SO_4)(OH)_6$, might be present in the samples, particular attention was paid to Sr lines, scanning the profile of spectral lines between Si and P peaks (Fig. 1*b*), where the energy maximum of Sr line (1.81 keV) occurs. The Sr line did not appear in any of the samples. A slightly raised background at 14 keV, where the Sr K_α peak is expected to appear, might suggest the presence of an insignificant amount of Sr, yet this determination is far from being reliable.

In one fragment nothing but Si was detected, which confirms the occurrence of quartz in phosphate aggregates. Most fragments contained only Fe, Mn, Ba, Pb (Fig. 1*a*). In these samples iron and manganese oxides and hydroxides coexisted, the latter being enriched in Ba and Pb.

From the spectrum shown in Fig. 1*b* it appears that besides the above-mentioned elements, the samples contain substantial amounts of Al, P and Si, a small amount

of Ca, and maybe also K. The presence of the latter is difficult to ascertain unequivocally, as the K K_α line lies close to the intense Ag L_α peak.

Titanium, which is detectable by spectroscopic method in an amount of 0.4%, failed to be detected with the electron microprobe because the strongest Ti K_α line (int. 100, 4.51 keV) lies close to the very intense Ba L_α line ((int. 100, 4.47 keV), and the weak Ti K_β line (int. 20, 4.93 keV) near the relatively intense Ba L_{β_1} line (int. 50, 4.83 keV). Therefore, Ti coincides with Ba which is the dominant constituent of the samples studied.

In view of the high Pb contents in the samples, an analysis of the Pb M_α peak, coinciding with sulphur, showed that sulphur was absent.

The spectrum presented in Fig. 1*b* was recorded for a mineral concentration consisting mainly of phosphates. It shows that also this sample is heterogeneous. The Si line has been attributed to quartz, the Fe and Mn, and partly Ba and Pb lines may be owing to the presence of Fe and Mn oxides and hydroxides (cf. spectrum la), whereas phosphates are responsible for P, Al, Ba, Ca and partly Pb lines.

Spectroscopic analysis was carried out on a high-resolution DFS-13 grating spectrograph in the region between 270 and 500 μm. The results obtained for the phosphate concentrate were compared with the data for manganese minerals from reniform concentrations. The principal components of phosphate concentrates were Ba, Al, Si and Fe, accompanied by substantial amounts, up to 0.4%, of Ti, Ca, Mg and Mn appeared as subordinate components. Moreover, the concentrates contained trace amounts of Pb (530—660 ppm), Zn (up to 760 ppm), V (100—180 ppm), Ni (40—80 ppm), Co (10—20 ppm), Sr (10—20 ppm). The elements present in amounts less than 10 ppm were Be, Zr, Ag, Mo, Cu, Sc, Ta, Nb, La.

In the comparative samples of manganese minerals, the contents of trace elements were quite different. Thus, Pb content ran up to 3% (specifically inside the reniform aggregates), Zn up to 1950 ppm, V up to 740 ppm, Ni up to 2300 ppm, Co up to 8600 ppm, Cu up to 1%, Ag up to 400 ppm, Mo up to 630 ppm. The Fe content varied from 0.5 to 1.2%. Sr appeared in trace amounts despite the fairly high Ba content (Kowalski, Chrostowska 1982). Characteristic were also very low Ti contents, of the order of 20 ppm.

The data obtained from all the chemical investigations suggest the following chemical composition of the phosphate in question. Its main components are Al, Ba and P. Ca, Mg and maybe also K are subordinate constituents, whereas Sr appears in trace amounts. The sample does not contain S. The presence of Fe and Mn, as well as of Pb, Co, Ni, etc., is to be attributed to an admixture of iron and manganese minerals. High Ti contents have been accounted for by the possibility of occurrence of a Ti mineral of the anatase type, yet mineralogical investigations failed to confirm its presence.

The cited data permit one to eliminate from the series of related phosphate minerals all those which contain Sr, Pb, Ca and SO_4^{2-} as principal components. It can be stated, therefore, that the phosphate under study is gorceixite with a slight Ca admixture. Its composition is close to that given by Povondra and Slánsky (1966), corresponding to the formula:

$$(Ba, Ca, Sr)Al_3(PO_4)_2(OH)_5 \cdot 2H_2O$$

The gorceixite from Stanisławów is primarily a barium-aluminium gorceixite.

X-ray diffraction patterns were recorded with a DRON-1 diffractometer, using filtered CuK_α and CoK_α radiation in the range of 2θ angles 4—65°. In order to check whether clay minerals occur in paragenesis with gorceixite, sedimented preparations were made for some samples, but X-ray investigations did not show their presence. All the X-ray diffraction patterns obtained were very similar to one another,

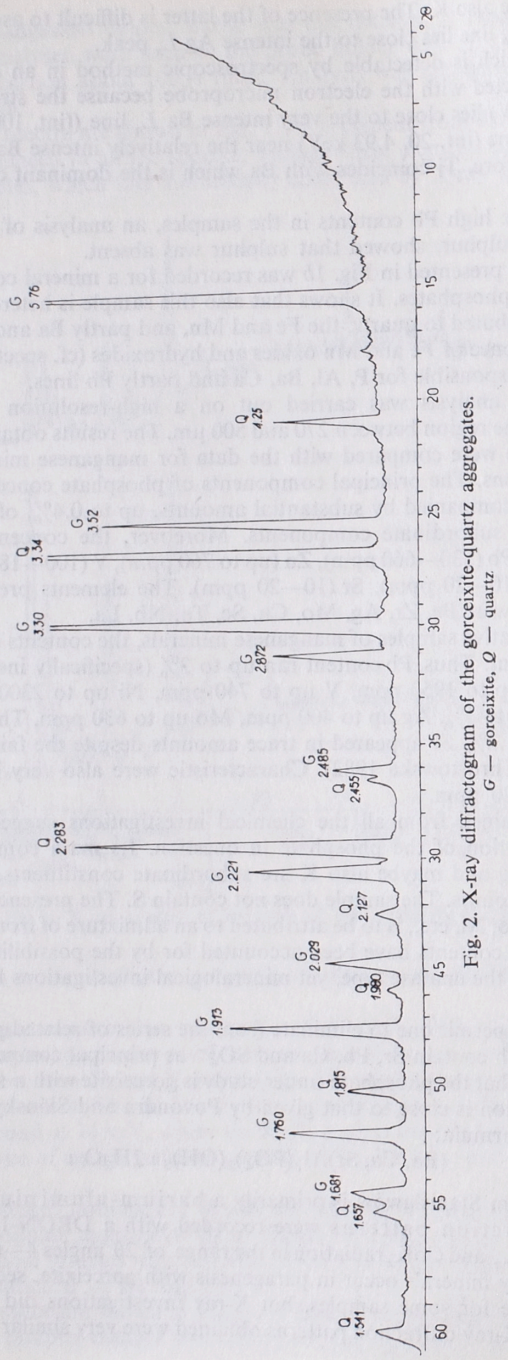

Fig. 2. X-ray diffractogram of the gorceixite-quartz aggregates. G — gorceixite, Q — quartz

differing only in the intensity of reflections according to the phosphate content in the concentrates. All the samples were found to contain quartz besides phosphate, and some of them iron oxides and hydroxides. Neither manganese oxides or oxyhydroxides nor titanium minerals were detected.

An X-ray diffraction pattern representative of the samples studied is shown in Fig. 2, and the interplanar spacings are given in Table 1. In this sample phosphate coexists with quartz.

The powder patterns recorded for the phosphate from Stanisławów show very close similarity to those obtained by Radoslovich and Slade (1980) for gorceixite from Glen Alice, NS Wales, corresponding to the crystallochemical formula:

$$(Ba_{0.95}, Sr_{0.01})\,Al_{3.02}(PO_4)_{2.01}(OH)_5 \cdot (H_2O)_{0.83}$$

Thermal analysis was carried out on an OD-102 derivatograph under the following conditions: temperature range 20—1050°C, sample 300 mg, TG sensitivity 100, DTA and DTG sensitivity 1/10, standard Al_2O_3, atmosphere of air, heating rate 10°C/min.

Figure 3 shows thermal curves obtained for the sample an X-ray diffractogram of which was presented in Fig. 2. The DTA curve (Fig. 3) shows the following thermal effects:

— a pronounced asymmetric endothermic effect with a peak at 600°C, the beginning of the effect at 400°C being relatively shallow and its end at 650°C very sharp.

Table 1

Interplanar spacings d_{hkl} (Å) of minerals occurring in the phosphate concentrate from Stanisławów

Phosphate concentrate Stanisławów		Gorceixite JCPDS (1972)		Gorceixite Radoslovich, Slade (1980)		Quartz Frondel (1962)	
d_{hkl}	I	d_{hkl}	I	d_{hkl}	I	d_{hkl}	I
5,76	70	5,73	90	5,753	90		
4,25	20					4,25	50
3,52	50	3,52	80	3,516	70		
3,34	80					3,34	100
3,00	100	2,978	100	3,002	100		
2,872	20	2,855	30	2,874	50		
2,485	10			2,488	50		
2,455	5	2,449	30			2,456	50
2,283	60	2,271	50	2,285	70	2,281	50
2,221	25	2,215	60	2,224	50	2,236	40
2,127	4					2,127	50
2,029	12	2,021	30	2,031	40		
1,980	2					1,980	40
1,913	30	1,905	70	1,913	70		
1,815	10					1,818	90
1,760	20	1,756	60	1,758	50		
1,681	10	1,675	20	1,681	40		
1,657	5	1,651	5			1,659	20
1,541	5					1,541	90

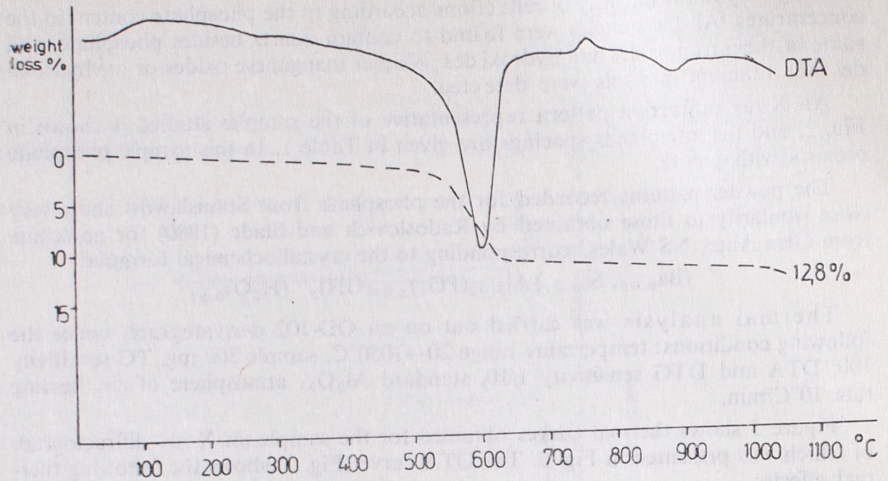

Fig. 3. Derivatogram of the gorceixite-quartz aggregates

The weight loss corresponding to this peak is substantial (9.3%) and has been accounted for by the loss of costitutional water;

— a less pronounced, diffuse endothermic effect with a peak at 895°C, without any significant weight loss. It has been ascribed to the decomposition of phosphate;

— very weak endothermic peaks at 285 and 390°C, presumably due to the continuous loss of adsorbed water;

— a pronounced exothermic peak at 760°C, associated with phase transition.

The total weight loss over the temperature range between 20 and 1050°C is 12.8%.

Žilcova, Ignatova and Karpova (1966) are of the opinion that typical of gorceixite are the endothermic peak at about 600°C and the weak exothermic effect between 800 and 900°C. Serduczenko and Czajka (1967) ascertained the continuous loss of water in gorceixite between 100 and 600°C with a peak at 400—580°C, and exothermic peaks at 820 and 960°C. Povondra and Slánsky (1966) noted for gorceixite endothermic peaks between 90 and 220°C, associated with the loss of adsorbed water, and endothermic effects at 470—520 and 530—580°C due to the loss of constitutional water. They ascribe the weak exothermic peaks at 850 and 1000°C to polymorphic transformation taking place in the phosphate. The thermal curves obtained for gorceixite from Stanisławów are similar to those presented by the cited authors.

Infrared spectroscopic analysis was carried out on a UR-20 spectrometer, using KBr disks. As appears from the spectrum shown in Fig. 4, the strongest absorptions at 1040, 1150 and 1060 cm^{-1} are caused by v_3 vibrations of $(PO_4)^{3-}$ anion. The latter band may be somewhat deformed due to the coincidence with the intense 1095 and 1168 cm^{-1} quartz bands lying in this region. However, the weak bands of relatively strong quartz absorption at 800 and 470 cm^{-1} indicate that the content of quartz in the analysed sample is very low and therefore should not have any significant effect on the deformation of the $(PO_4)^{3-}$ absorption. The v_4 vibration of $(PO_4)^{3-}$ anion gives rise to the bands of lower intensity at 515 and 590 cm^{-1}. The $(PO_4)^{3-}$ anion is also responsible for the weak absorptions at 820 and 900 cm^{-1}. The intense absorption between 3620 and 3760 cm^{-1} was attributed to $(OH)^-$ stretching vibra-

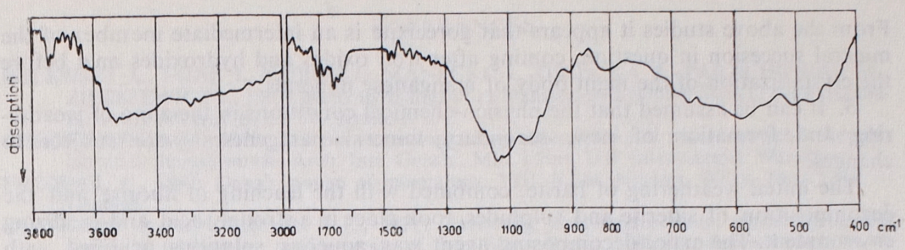

Fig. 4. Infrared absorption spectrum of gorceixite from Stanisławów

tions. Absorption bands corresponding to H_2O vibration occur at 1600—1650 cm^{-1}. H_2O molecules also give rise to broad, diffuse bands between 3000 and 3600 cm^{-1}. In this region the 3450 cm^{-1} band occurs, arising from OH stretching vibration.

Thermal and infrared spectroscopic analyses have shown that both H_2O molecules and $(OH)^-$ groups are present in the phosphate studied.

DISCUSSION

1. Chemical and mineralogical investigations have shown that the phosphate found in the weathering zone of a barite-fluorite deposit at Stanisławów is gorceixite. Its principal components are Ba, Al, (PO_4) and (OH) groups, and H_2O. It also contains a small amount of Ca and trace amounts of Mg, Sr, K, Pb, Zn, V, Co, Ni, etc. It can be defined, therefore, as Ca-and Sr-poor barium-aluminium gorceixite, corresponding to the crystallochemical formula given by Povondra and Slansky (1966):

$$(Ba, Ca, Sr)Al_3(PO_4)_2(OH)_5 \cdot 2H_2O$$

A similar formula for gorceixite was given by Radoslovich and Slade (1980).

2. The gorceixite from Stanisławów forms very fine-crystalline aggregates. Its crystals are characterized by a prismatic or rhombohedral habit, showing commonly a zonal structure. The crystal habit suggests trigonal symmetry. This statement is in accordance with the data published by Radoslovich and Slade, who have found that gorceixite has pseudotrigonal symmetry resulting from polysynthetic twinning of uniaxial crystals.

3. The gorceixite from Stanisławów occurs in the weathring zone of a barite-fluorite deposit in paragenesis with iron oxides and hydroxides, automorphic transparent barite, reniform manganese minerals of the hollandite-coronadite type, and with lithiophorite. Gorceixite aggregates always contain quartz and have an increased Ti content, which suggests the occurrence of a titanium mineral of the anatase type. This mineral failed, however, to be detected by the methods used.

4. The following regularities emerge from the study of the mineral succession in the weathering zone of the Stanisławów deposit: Iron oxides and hydroxides were the first to precipitate on altered barite and in cavities formed within the barite. They formed incrustations of various kinds and hard, irregular concentrations resembling slags and sinters, frequently occurring independently. Yet in other parts of the deposit automorphic, transparent barite crystals grow on iron minerals, interfingering with gorceixite. The latter passes into brecciated manganese aggregates which are the initial stage of their crystallization. The principal stage of crystallization of manganese aggregates gave rise to nodular concentrations of these minerals, sometimes up to 30 cm in diameter. Their surface is generally coated with a thin layer of lithiophorite.

From the above studies it appears that gorceixite is an intermediate member of the mineral succesion in question, coming after iron oxides and hydroxides and before the crystallization of the main body of manganese minerals.

5. It can be assumed that the physico-chemical conditions in the zone of weathering and formation of new, secondary mineral parageneses were subject to changes.

The initial weathering of barite, combined with the leaching of fluorite and the decomposition of siderite and sulphides, took place in a strongly acid and oxidizing environment. The major decomposing agent was aqueous solutions acidified with sulphuric acid deriving from iron sulphates which were common both in the deposit and the enclosing rocks. As the environment was progressively changing to alkaline, the main mass of iron oxide and hydroxide minerals precipitated. The crystallization of automorphic barite, as well as of gorceixite, with the co-precipitation of titanium compounds took place presumably in an environment with pH 6—8. The studies of Serduczenko and Czajka (1967) point to similar conditions of the crystallization of gorceixite. According to these authors, gorceixite crystallizes at pH about 7 and in certain parageneses its crystallization follows kaolinization and the crystallization of barite. Basing on the experimental evidence, Żilcova et al. (1966) found that gorceixite formed at pH 5.88—6.75 and 8.72—10.20. The crystallization of the main body of manganese minerals took place in a strongly alkaline environment. The studies of Kowalski (1977) showed that the crystallization of automorphic, transparent barite occurred over a temperature range of 30—50°C, and it can be assumed that also gorceixite formed under such conditions.

6. Gorceixite and the related phosphates are minerals typical of weathering zones.

In the environment very similar to that at Stanisławów occurs gorceixite described by Serduczenko and Czajka (1967) from iron-manganese weathering wastes from Czadobińsk in Siberia, where it is found in association with barite, rutile and kaolinite. Povondra and Slánsky (1966) found gorceixite in argillitized phonolites of the Host-Chomotov-Teplice basin, where it coexisted with haematite, goethite, quartz and anatase. These authors also studied gorceixite from diamond-bearing sands of Riodbaete, Brazil. Loughnan and Ward (1970) described gorceixite from kaolinitized diabases and basalts from Glen Alice in NS Wales, where it forms parageneses with kaolinite, quartz, anatase, siderite, goyasite, crandallite and florencite. Goldbery and Loughnan (1977) reported gorceixite from Permian marine deposits of the Sydney basin, Australia, from parageneses with dawsonite, alumohydrocalcite and nordstrandite.

In Poland, svanbergite and hindsdallite, i.e. phosphates related to gorceixite, were described from Lower Silesian kaolins (Szpila, Dzierżanowski 1978), and crandallite e.g. from a basaltic weathering waste in a brown coal mine at Turoszów (Szpila, Stępisiewicz 1979). In these localities the phosphates were always accompanied by titanium oxide minerals.

7. The source of elements for the new-formed minerals in the weathering zone of the Stanisławów barite deposit were both barite-fluorite ores and the weathering wall rocks. Iron and manganese derived primarily from the decomposition of siderites which occurred locally in the ores in substantial amounts, and contained on the average 7.4% $MnCO_3$ (Paulo 1972, Kowalski 1980). The authors believe that Ba and Pb also had their source in the deposit. Other elements were presumably derived from the host rocks in which apatite is very common and the content of Ti averages 0.5—1.9%, that of Co 13—31 ppm, Ni 30—35 ppm, V 80—165 ppm, Cu 28—70 ppm (Kowalski 1977).

Translated by Hanna Kisielewska

REFERENCES

BOLEWSKI A., FIJAŁ J., KUBISZ J., MANECKI A., OSZACKA B., PARACHONIAK W., ZIĘTKIEWICZ J., 1969: Minerały manganu ze Stanisławowa (Dolny Śląsk) i ich paragenеza. *Prace Mineralogiczne 20.* Kraków.

CHROSTOWSKA M., 1970: Badania mineralogiczno-geochemiczne rud manganowych w kopalni barytu w Stanisławowie. Arch. Inst. Geoch., Min. i Petr. UW (manuscript). Warszawa.

FRONDEL C., 1962: Dana's system of mineralogy. VIII. Silica minerals. Wiley. New York — London.

GOLDBERY R., LOUGHNAN F. C., 1977: Dawsonite, alumohydrocalcite, nordstrandite and gorceixite in Permian marine strata of the Sydney Basin, Australia. *Sedimentology* 24, 4. Zürich.

JCPDS, 1972: Joint Committee on Powder Diffraction Standards. After: Povondra, Slánsky (1966).

JERZMAŃSKI J., 1965: Budowa geologiczna północno-wschodniej części Gór Kaczawskich i ich wschodniego przedłużenia. *Biul. IG* 185.

JERZMAŃSKI J., KORNAŚ J., 1970: Minerały złoża barytu w Stanisławowie na Dolnym Śląsku. *Prace IG* 59.

[KASZKAJ M. A.] КАШКАЙ М. А., 1970: Алуниты, их генезис и исспользование. Т. I. Нерда. Москва.

KOWALSKI W., 1967: Wyniki badań mineralogiczno-geochemicznych rud manganowych z kopalni barytu w Stanisławowie. Arch. Inst. Geoch., Min. i Petr. UW (manuscript). Warszawa.

KOWALSKI W., 1977: Geochemia, mineralogia i geneza dolnośląskich złóż i wystąpień barytowych. Cz. II. *Arch. Miner.* 33, 1.

KOWALSKI W., 1980: Badania mineralogiczno-geochemiczne złoża barytowo-fluorytowego w Stanisławowie w Górach Kaczawskich. Arch. Inst. Geoch., Min. i Petr UW (manuscript). Warszawa.

KARWOWSKI Ł., KOWALSKI W., 1981: Sulfide minerals from the barite-fluorite deposit at Stanisławów in the Kaczawa Mts., Lower Silesia. *Acta Geol. Pol.* 31, 1—2.

KOWALSKI W., CHROSTOWSKA-STRZESZEWSKA M., 1982: Paragenezy mineralne strefy wietrzenia złoża barytowo-fluorytowego w Stanisławowie (*in press*).

LOUGHNAN F. C., WARD C. R., 1970: Gorceixite-goyazite in kaolinite rocks of the Sydney Basin. *Journ. Prof. Soc. New South Wales*, 103.

PAULO A., 1972: Charakterystyka mineralogiczna złoża barytu w Stanisławowie (Dolny Śląsk). *Prace Mineralogiczne* 29. Kraków.

PAULO A., 1973: Złoże barytu w Stanisławowie na tle metalogenii Gór Kaczawskich. *Prace Geologiczne* 76. Kraków.

POVONDRA P., SLÁNSKY E., 1966: Occurrence of gorceixite in argillized phonolites of northwestern Bohemia. *Acta Univ. Carolinae*, 1. Praha.

RADOSLOVICH E. W., SLADE E., 1980: Pseudo-trigonal symmetry and the structure of gorceixite. N. *Jb. Miner. Mh.*, 4.

[SERDUCZENKO D. P. CZAJKA M. W.] СЕРДУЧЕНКО Д. П., ЧАЙКА В. М., 1967: Геохимическая история фосфора и бария при формировании карбонатоподобных пород и древных кор выветривания Чадобецкого поднятия. *Доклады АН СССР* 117, 4.

SZPILA K., DZIERŻANOWSKI P., 1978: Minerały typu svanbergitu i hinsdalitu w kaolinach. Mat. z I. Konf.: Minerały i surowce ilaste. Bolesławiec.

SZPILA K., STĘPISIEWICZ M., 1979: Phosphate minerals in basaltic weathering products from Turoszów (Lower Silesia). *Arch. Miner.* 35, 2. Warszawa.

[ŻILCOWA I. A., IGNATOWA L. J., KARPOWA L. N.] ЖИЛЬЦОВА И. Г., ИГНАТОВА Л. И., КАРПОВА Л. Н., 1966: Получение искуственного горцеиксита. В кн.: Исследование природных и технических минералообразцов. Москва.

Włodzimierz KOWALSKI, Ilona ŚMIETAŃSKA

GORCEIXYT ZE ZŁOŻA BARYTOWO-FLUORYTOWEGO W STANISŁAWOWIE (GÓRY KACZAWSKIE)

Streszczenie

Metodami chemicznymi oraz analizy fazowej stwierdzono w strefie wietrzenia złoża barytowo-fluorytowego w Stanisławowie występowanie gorceixytu. Zidentyfikowano go jako gorceixyt barowo-glinowy, zawierający tylko bardzo drobne domieszki Ca i Sr. Jego wzór krystalochemiczny można przedstawić następująco:

$$(Ba, Ca, Sr)Al_3(PO_4)_2(OH)_5 \cdot 2H_2O.$$

Gorceixyt tworzy agregaty drobnokrystalicznych osobników przerastających się z kwarcem. W agregatach tych stwierdzono znaczne zawartości Ti dochodzące do 0,4%.

W paragenezie z gorceixytem współwystępują tlenki i wodorotlenki żelaza, automorficznie wykształcony baryt, naciekowe formy skupień minerałów manganowych typu hollandytu-koronadytu oraz pylasty litioforyt.

Źródłem pierwiastków dla nowopowstałych paragenez mineralnych strefy wietrzenia były zarówno rudy barytowo-fluorytowe, jak również wietrzejące skały osłony złoża.

Ustalono, że gorceixyt tworzył się w środowisku utleniającym, przy pH w granicach 6—8 i temperaturze 30—50°C.

OBJAŚNIENIA FIGUR

Fig. 1. Widma rentgenowskie minerałów paragenezy gorceixytowej

Fig. 2. Dyfraktogram agregatów gorceixytu z kwarcem
G — gorceixyt, *Q* — kwarc

Fig. 3. Derywatogram agregatów gorceixytu z kwarcem

Fig. 4. Widmo absorpcyjne w podczerwieni gorceixytu ze Stanisławowa

OBJAŚNIENIA FOTOGRAFII

Plansza I

Fot. 1. Gniazdowe skupienia agregatów gorceixytowo-kwarcowych (jasne plamy) występujące w podstawie brekcjowato wykształconych nacieków manganowych. Dolna partia nacieków (szara) jest bardziej żelazista, natomiast górna (czarna) prawie wyłącznie manganowa. Pow. 2×. Fot. A. Pelc

Fot. 2. Gniazdowe skupienia agregatów gorceixytowo-kwarcowych (jasne plamy) w podstawie nacieków manganowych. Pow. 2×. Fot. A. Pelc

Plansza II

Fot. 3. Gniazdowe skupienia agregatów gorceixytowo-kwarcowych (jasne plamy) w podstawie nacieków manganowych. Pow. 2×. Fot. A. Pelc

Fot. 4. Obrazy mikroskopowe gorceixytu w skupieniach z kwarcem (jaśniejsze, większe ziarna). Niektóre osobniki gorceixytu wykazują budowę zonalną. W czarnych miejscach występują głównie minerały manganu. 1 nikol. Pow. 480×. Fot. I. Śmietańska

Plansza III

Fot. 5. Obrazy mikroskopowe gorceixytu w skupieniach z kwarcem (jaśniejsze, większe ziarna). Niektóre osobniki gorceixytu wykazują budowę zonalną. W czarnych miejscach występują głównie minerały manganu. 1 nikol. Pow. 480×. Fot. I. Śmietańska

Fot. 6. Skupienia tabliczkowo wykształconych osobników gorceixytu. SEM, pow. 1400×. Fot. E. Klichowicz

Plansza IV

Fot. 7. Skupienie gorceixytu. Występujący w środku skupienia kryształ o wielkości około 0.03 mm wykazuje wyraźną symetrię trygonalną. SEM, pow. 2000×. Fot. E. Klichowicz

Fot. 8. Skupienie gorceixytu. Pokrój osobników słupkowo-romboedrycznych. Największe ziarna osiągają 0,05—0,06 mm średnicy. SEM, pow. 800×. Fot. E. Klichowicz

Влодзимеж КОВАЛЬСКИ, Илёна СЬМЕТАНЬСКА

ГОРСЕЙКСИТ ИЗ БАРИТ-ФЛЮОРИТОВОГО МЕСТОРОЖДЕНИЯ В СТАНИСЛАВОВЕ (КАЧАВСКИЕ ГОРЫ)

Резюме

Химическими методами, а также фазовым анализом, было обнаружено присутствие горсейксита в зоне выветривания барит-флюоритового месторождения в Станиславове. Он был определен как барий-алюминиевый горсейксит, содержащий лишь очень небольшие примеси Ca и Sr. Его кристаллохимическую формулу можно представить следующим образом:

$$(Ba, Ca, Sr)Al_3(PO_4)_2(OH)_5 \cdot 2H_2O.$$

Горсейксит образует агрегаты срастающихся с кварцем мелкокристаллических индивидов. Кроме того, в этих агрегатах обнаружено значительное содержание Ti до 0,4%.

В парагенезе с горсейкситом совместно встречаются: окислы и гидроокислы железа, идиоморфного габитуса барит, натечные формы скоплений марганцевых минералов типа голландит-коронадита, а также пылеватый литиофорит.

Источником химических элементов для новообразующихся минеральных парагенезов коры выветривания были как барит-флюоритовые руды, так и подвергающиеся выветривании вмещающие породы.

Установлено, что горсейксит образовалса в окислительной обстановке при pH в пределах 6—8 и в температуре 30—50°C.

ОБЬЯСНЕНИЯ К ФИГУРАМ

Фиг. 1. Рентгеновские спектры минералов горсейкситового парагенеза

Фиг. 2. Дифрактограмма агрегатов горсейксита с кварцем
G — горсейксит, *Q* — кварц

Фиг. 3. Дериватограмма агрегатов горсейксита с кварцем

Фиг. 4. ИК-спектр горсейксита из Станиславова

ОБЪЯСНЕНИЯ К ФОТОГРАФИЯМ

Таблица I

Фото 1. Гнездовые скопления горсейксит-кварцевых агрегатов (светлые пятна), развитые в основании брекчиевидных марганцевых натеков. Нижняя часть натеков (серая) более железиста, верхняя же (черная) почти исключительно марганцева. Увел. × 2. Фото А. Пэльц

Фото 2. Гнездовые скопления горсейксит-кварцевых агрегатов (светлые пятна) в основании марганцевых натеков. Увел. × 2 Фото А. Пэльц

Таблица II

Фото. 3. Гнездовые скопления горсейксит-кварцевых агрегатов (светлые пятна) в основании марганцевых натеков. Увел. × 2. Фото А. Пэльц

Фото. 4. Микроскопическая картина горсейксита в скоплениях с кварцем (более светлые и крупные зерна). Некоторые индивиды горсейксита обнаруживают зональное строение. В черных пятнах развиты главным образом марганцевые минералы. Один николь. Увел. × 480. Фото И. Сьметаньска

Таблица III

Фото 5. Микроскопическая картина горсейксита в скоплениях с кварцем (более светлые и крупные зерна). Некоторые индивиды горсейксита обнаруживают зональное строение. В черных пятнах развиты главным образом марганцевые минералы. Один николь. Увел. × 480. Фото И. Сьметаньска

Фото 6. Скопления таблитчатых индивидов горсейксита. РЭМ, увел. × 1400 Фото Э. Клихович

Таблица IV

Фото 7. Скопление горсейксита. Развитый в центре скопления кристалл размером около 0,03 мм обнаруживает явную тригональную сингонию. РЭМ, увел. × 2000 Фото Э. Клихович

Фото 8. Скопление горсейксита призматическо-ромбоэдрического габитуса. Наиболее крупные зерна достигают 0,05—0,06 мм в диаметре. РЭМ, увел. × 800. Фото Э. Клихович

Phot. 1. Nest-like concentrations of gorceixite-quartz aggregates (light spots) occurring at the base of brecciated manganese concentrations. The lower part of concentrations (grey) has a higher iron content while the upper part (black) consists almost entirely of manganese. 2×. Phot. A. Pelc

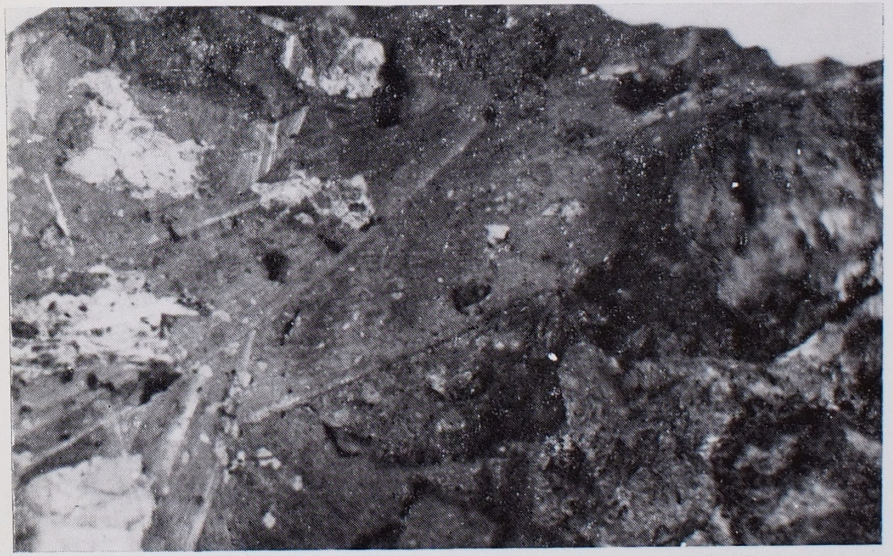

Phot. 2. Nest-like concentrations of gorceixite-quartz aggregates (light spots) at the base of manganese concentrations. 2×. Phot. A. Pelc

Włodzimierz KOWALSKI, Ilona ŚMIETAŃSKA — Gorceixite from a barite-fluorite deposit at Stanisławów (Kaczawskie Mts.)

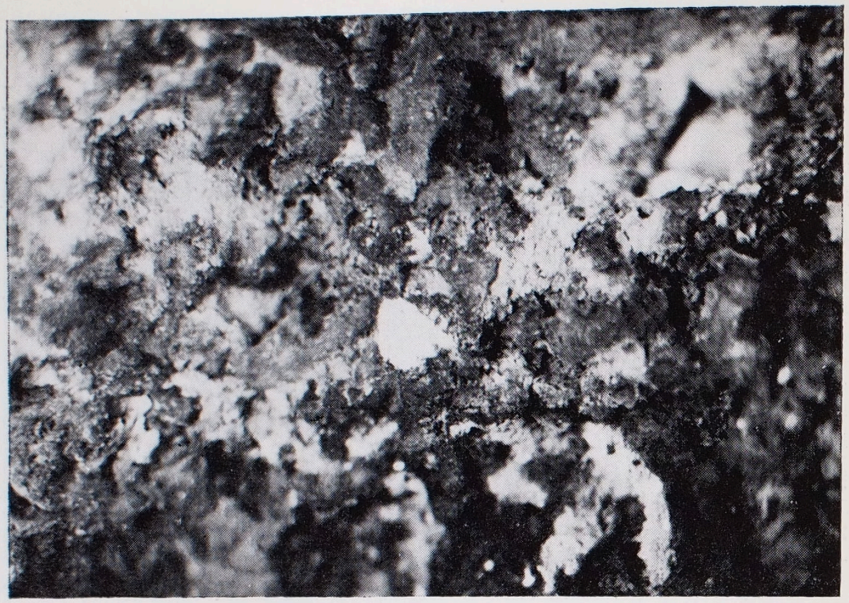

Phot. 3. Nest-like concentrations of gorceixite-quartz aggregates (light spots) at the base of manganese concentrations. 2×. Phot. A. Pelc

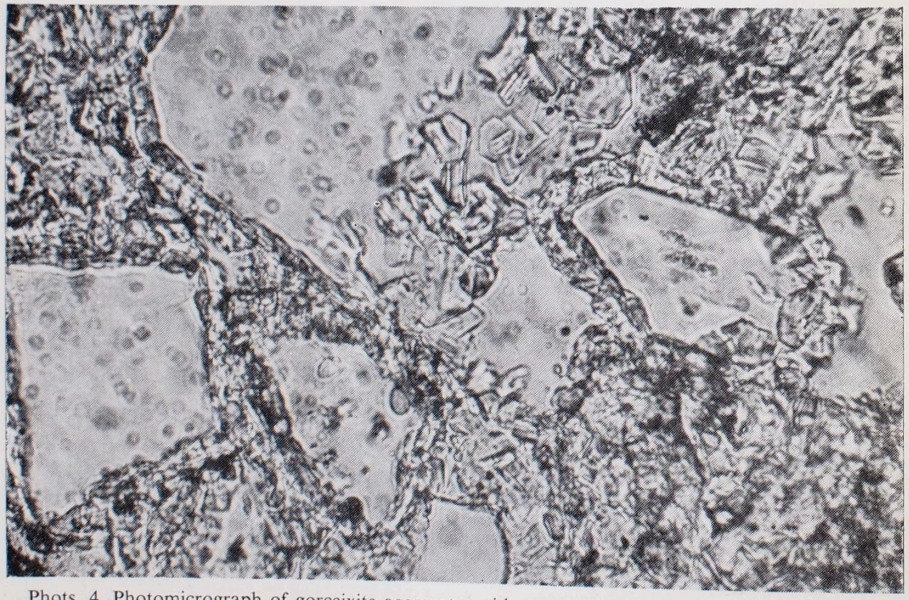

Phots. 4. Photomicrograph of gorceixite aggregates with quartz (lighter, larger grains). Some gorceixite crystals show a zonal structure. In black places there occur mainly manganese minerals. Polarized light, 1 nicol, 480×. Phot. I. Śmietańska

Włodzimierz KOWALSKI, Ilona ŚMIETAŃSKA — Gorceixite from a barite-fluorite deposit at Stanisławów (Kaczawskie Mts.)

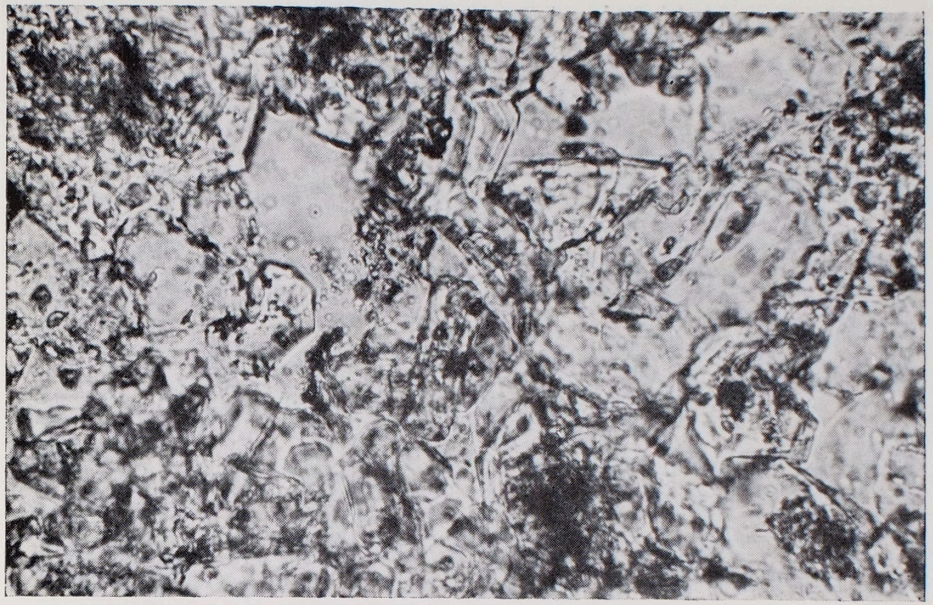

Phot. 5. Photomicrograph of gorceixite aggregates with quartz (lighter, larg grains). Some gorceixite crystals show a zonal structure. In black places there occur mainly manganese minerals. Polarized light, 1 nicol, 480×. Phot. I. Śmietańska

Phot. 6. Aggregates of tabular gorceixite crystals. SEM, 1400×. Phot. E. Klichowicz

Włodzimierz KOWALSKI, Ilona ŚMIETAŃSKA — Gorceixite from a barite-fluorite deposit at Stanisławów (Kaczawskie Mts.)

Phot. 7. Gorceixite aggregate. A crystal in the centre of aggregate, about 0.03 mm in size, shows distinct trigonal symmetry. SEM, 2000×. Phot. E. Klichowicz

Phot. 8. Gorceixite aggregate. Crystals exhibit a prismatic-rhombohedral habit. Largest grains are 0.05—0.06 mm in diameter. SEM, 800×. Phot. E. Klichowicz

Włodzimierz KOWALSKI, Ilona ŚMIETAŃSKA — Gorceixite from a barite-fluorite deposit at Stanisławów (Kaczawskie Mts.)